Biogeography and diversification rates in hornworts: The limitations of diversification modeling

Article *in* Taxon · February 2015

DOI: 10.12705/642.7

3 authors:

Juan Carlos Villarreal
Laval University
77 PUBLICATIONS **1,434** CITATIONS
SEE PROFILE

Natalie Cusimano
Ludwig-Maximilians-University of Munich
31 PUBLICATIONS **474** CITATIONS
SEE PROFILE

Susanne S. Renner
Ludwig-Maximilians-University of Munich
456 PUBLICATIONS **9,862** CITATIONS
SEE PROFILE

Biogeography and diversification rates in hornworts: The limitations of diversification modeling

Juan Carlos Villarreal, Natalie Cusimano & Susanne S. Renner

Systematic Botany and Mycology, Department of Biology, University of Munich (LMU), Menzingerstr. 67, 80638 Munich, Germany
Author for correspondence: *Juan Carlos Villarreal, jcarlos.villarreal@gmail.com*
ORCID: JCV, http://orcid.org/0000-0002-0770-1446

DOI http://dx.doi.org/10.12705/642.7

Abstract Hornworts comprise ca. 220 species and are among the oldest landplant lineages, even though their precise phylogenetic position remains unclear. Deep within-hornwort divergences, highly uneven species numbers per genus, and the assumed high stem age together suggest a history of changing diversification (i.e., speciation minus extinction) rates. To study the geographic distribution of modern hornworts and their patterns of species accumulation, we generated a mitochondrial and plastid DNA matrix for 103 species representing all major groups and then applied molecular-clock dating, using a different calibration approach than in earlier work. We used the BAMM software to fit rate-variable and constant-rate birth-death diversification models to the dataset, and we also inferred ancestral areas to a time depth of 55 Ma (Early Eocene). We analyzed diversification rates for all hornworts and separately for species-rich subclades. Under BAMM's variable-rates model (which fits the data better than a constant-rate birth-death model, but still assumes that each species has the same speciation and extinction probability regardless of its age), hornworts have gradually increasing rates of speciation and a constant background extinction rate. No shifts in diversification rate could be detected. The implausible finding of a constant background extinction rate illustrates the limitations of diversification modeling especially as regards extinction rates.

Keywords biogeography; diversification modeling; extinction rates; geographic disjunctions; hornworts

Supplementary Material The Electronic Supplement (Fig. S1) is available in the Supplementary Data section of the online version of this article at http://www.ingentaconnect.com/iapt/tax

■ INTRODUCTION

Hornworts comprise ca. 220 species worldwide. In spite of large-scale efforts, molecular data have so far not solved their precise relationships to other land plants (Qiu & al., 2006; Karol & al., 2010; Wickett & al., 2014). A recent re-analysis of earlier DNA data suggested that bryophytes (hornworts, liverworts, mosses) might be monophyletic (Cox & al., 2014), but Wickett & al. (2014), using up to 852 nuclear genes from 92 species across green organisms, two of them hornworts, again failed to resolve the placement of hornworts as either sister to all other land plants or as a member of a bryophyte monophylum. Given the undoubted high geological age of all three bryophyte lineages, biogeographic reconstruction is problematic because continental positions and climates have changed dramatically over the past hundred million years (Scotese, 2001). Nevertheless, one can infer ancestral areas for more "shallow" nodes reflecting diversification events that took place over the Pliocene, Miocene or Oligocene. For example, a study focusing on the Neotropical hornwort genus *Nothoceros* (R.M.Schust.) J.Haseg. inferred a crown group age of ca. 35 Ma (Villarreal & Renner, 2014, using a plastid rate calibration) and a split between *N. endiviifolius* (Mont.) J.Haseg. from Chile and its sister species *N. giganteus* (Lehm. & Lindenb.) J.Haseg. from New Zealand at 5.3 Ma or 20.7 Ma, depending on the calibration used. These ages imply long-distance dispersal, even in the face of great dating uncertainty.

Spore-producing plants, such as bryophytes, lycophytes and ferns, may be particularly prone to long-distance dispersal (Muñoz & al., 2004). In hornworts, spore sizes range from 18 µm diameter in *Leiosporoceros* Hässel to >100 µm in the multicellular spores of the epiphytic *Dendroceros* Nees (Renzaglia & al., 2009), and such small, wind-borne spores may travel far. The flagellate sperm cells, however, travel only a few centimeters (Proskauer, 1948), and many species are dioicous, meaning that they require at least two different-sexed individuals for a new population to become established after long-distance dispersal. In an earlier study, we carried out trait reconstruction, focusing on sexual systems, spore sizes, and antheridium number, on a phylogeny for 98 species of hornworts that represented roughly equal proportions of the monoicous and dioicous species, and the results revealed that diversification rates, which reflect the difference between speciation and extinction, do not correlate with sexual systems (Villarreal & Renner, 2013). In that study, we relied on the binary-state speciation and extinction (BISSE) model

Received: 30 Nov 2014 | returned for (first) revision: 25 Jan 2015 | (last) revision received: 1 Feb 2015 | accepted: 3 Feb 2015 || publication date(s): online fast track, n/a; in print and online issues, 6 May 2015 ||

(Maddison & al., 2007; FitzJohn & al., 2009). This method estimates trait-dependent speciation and extinction rates in a Bayesian framework, the binary character in our case being sexual system (but see Maddison & Fitzjohn, 2015 and Rabosky & Goldberg, 2015 for statistical problems with this model).

Clearly, the species-poverty of hornworts, with only about 220 species worldwide, poses a problem for statistical diversification analyses, all of which rely on the relative distribution of nodes in ultrametric trees (e.g., clock-dated phylogenies). For more species-rich spore-producing plants, such as ferns, mosses, or liverworts, changes in diversification rates over time have been associated with fluctuating global climates or the rise of the angiosperms (Schneider & al., 2004; Schuettpelz & Pryer, 2009; Fiz-Palacios & al., 2011), and one might expect similar patterns in hornworts. A study by Laenen & al. (2014), comparing diversification rates in liverworts, mosses, and hornworts, however, found that a model of constant diversification through time could be rejected in mosses and liverworts but not in hornworts because of the lack of statistical power associated with the small number of included hornworts (their data matrix included one species per genus). They nevertheless reported high diversification rates in hornworts, especially for *Anthoceros* L.–*Sphaerosporoceros* Hässel. The model used by Laenen & al. was MEDUSA, a maximum likelihood method for modeling among-lineage heterogeneity in speciation-extinction dynamics (Alfaro & al., 2009). Experimental work since 2009 has shown that MEDUSA consistently underestimates the true number of processes in simulated datasets when rates of speciation vary through time and that branch-specific speciation rates estimated with MEDUSA show little correspondence with true rates (Rabosky, 2014). This may not be a problem when data meet the assumption that rates of species diversification are constant in time, but it may become a problem where this assumption is violated.

Here, we study clade age, diversification, and biogeography of hornworts, using a DNA data matrix that includes all genera represented by 103 of their combined 220 species. In representing at least one species of each genus, our matrix is not randomly sampling hornwort diversity. Nevertheless, the signal in a tree with 102 nodes might be able to reject a constant rate of diversification through time, different from the few hornwort species in the Laenen & al. (2014) tree. We used the BAMM software, which fits four diversification models (time-dependent, diversity-dependent, and constant-rate pure birth or birth-death) to ultrametric trees and which has been shown to outperform MEDUSA (Rabosky, 2014). The program works well with trees as small as 87 tips (as in the files distributed with the software), although power to detect rate variation decreases in small trees. BAMM infers changes in diversification rate along branches (each branch, of course, influenced by neighboring branches/clades), statistically adds missing species, and to some extent can account for non-random species sampling (Rabosky, 2014). It is well known that incomplete taxon sampling can bias analyses of speciation and extinction from phylogenetic trees, at least if the included species are not a random sample of the clade of interest, but instead selected to represent the oldest, most diverse taxa and/or one representative of each subtaxon of the focal clade (Cusimano & Renner, 2010; Cusimano & al., 2012). For such situations, BAMM permits the user to specify the percentage of species that have been sampled. Users can also specify clade-specific sampling fractions if the percentage of sampled taxa varies considerably across a tree. The main questions we wanted to answer were, (1) what is the geographic distribution of the major hornwort lineages worldwide (a question not addressed in previous studies) and (2) does a phylogeny with about 50% of the extant species (102 nodes) reveal a signal of changing diversification through the clade's long history, when analyzed with the most powerful current diversification modeling?

■ MATERIALS AND METHODS

Taxon sampling, DNA sequencing, and phylogenetic analysis. — We sequenced 103 species of hornworts, including 5 new ones (Appendix 1), for the mitochondrial *nad5* exon2 and the plastid regions *rbcL*, *trnK* including *matK*, and *rps4*. Primers for the *rps4* region were newly designed based on the two available plastid hornwort genomes (Villarreal & al., 2013): rps40F 5′ TCGTCTGGGGACTCTACCAG 3′ and rps540R 5′ AACCAATCCAGTCACGATCT 3′. Primers for the other DNA regions are given in Villarreal & Renner (2013), and PCR protocols followed standard procedures. Sequence editing and alignment were carried out in Geneious v.5.6.6 (Biomatters, Auckland, New Zealand) and the alignment has been deposited in TreeBase (http://treebase.org/treebase-web/, study accession number 17263). In the absence of statistically supported (e.g., >95% bootstrap support) topological contradiction, the mitochondrial and plastid data matrices were concatenated, yielding an alignment of 4182 nucleotides. Phylogenetic analyses were performed under likelihood optimization and the GTR+Γ substitution model, using RAxML v.7.2.8 (Stamatakis & al., 2008) with 100 bootstrap replicates under the same model. All analyses were run using the Cipres Science Gateway servers. Trees were rooted on *Leiosporoceros dussii* (Steph.) Hässel, the sole species of Leiosporocerotaceae, which is sister to all other hornworts (Duff & al., 2007; Villarreal & Renner, 2012).

Molecular clock dating. — We used two calibration approaches. First, we used *Notothylites nirulai* Chitaley & Yawale from the Deccan Intertrappean beds of Mohgaonka, India (Maastrichtian, 65–70 Ma; Chitaley & Yawale, 1980) to constrain the age of the stem node of *Notothylas* Sull. ex A.Gray and *Phaeoceros* Prosk. (including *Paraphymatoceros* Hässel). This petrified fossil of an entire plant has similar thallus size, sporophyte size, and elater shape to extant *Notothylas*. In the present paper, we gave this fossil a lognormal prior with a median of 77 Ma and an offset of 65 Ma; this lets 95% of the ages fall between 67 and 127 Ma. In a previous study, we used an exponential prior with a median of 131 and an offset of 65 Ma, which let 95% of the ages fall between 70 and 351 Ma (Villarreal & Renner, 2012). Second, we used a substitution rate of 5.0×10^{-4} substitutions/site/Myr from the entire single-copy region and inverted repeats of land plants (Palmer, 1991) for the plastid data partition and a rate of

1.9×10^{-4} substitutions/site/Myr (Gaut, 1988) for the mitochondrial data partition. Different from an earlier study (Villarreal & Renner, 2012), we here refrain from including land plant outgroups because (1) bryophytes may be monophyletic after all (Cox & al., 2014) and (2) the inclusion of sparse outgroups violates a basic assumption of Bayesian dating approaches, namely even taxon sampling across lineages (Drummond & Bouckaert, 2015). As explained above, we instead rooted on *Leiosporoceros*.

Dating relied on Bayesian divergence time estimation as implemented in BEAST v.1.8.1 (Drummond & al., 2012), using a Yule tree prior (as appropriate for our sampling of one plant per species) and the GTR+Γ substitution model with unlinked data partitions to account for the mitochondrial and plastid data. The fossil calibration was applied both in a strict clock model and an uncorrelated log-normal (UCLN) relaxed clock model, while the rate calibration was only applied in the strict clock. MCMC chains were run for 100 million generations, with parameters sampled every 10,000th generation. Tracer v.1.6 (Rambaut & al., 2014) was used to assess effective sample sizes (ESS) for all estimated parameters and to decide the appropriate percentages of burn-in. We verified that all ESS values were >200. Trees were combined in TreeAnnotator v.1.6.1 (part of the BEAST package), and maximum clade credibility trees with mean node heights were visualized using FigTree v.1.40 (Rambaut, 2014). We report highest posterior densities (HPD) intervals (the interval containing 95% of the sampled values).

Ancestral area reconstructions. — We performed maximum likelihood (ML) ancestral area reconstruction in Mesquite v.2.73 (Maddison & Maddison, 2010) with the Mk1 model and the fossil-calibrated UCLN chronogram as input tree. Distribution data were obtained mainly from Hasegawa (1980), Asthana & Srivastava (1991), and Piippo (1993). We coded species for their occurrence in the following regions (based on the provenance of the sequenced specimen): A, tropical Africa and/or tropical Asia between 25° N and S lat.; B, tropical America between 25° N and S lat.; C, Eurasia and America north of 25° N lat. ("North Temperate"); and D, South America, Australia and New Zealand south of 25° S lat. ("South Temperate"). We only report inferences to a time depth of up to 55 Ma because of vastly different continental positions and climates prior to the Eocene (and even since then; Scotese, 2001).

Diversification analyses. — To assess diversification patterns, we relied on BAMM v.1.0 (Rabosky, 2014). We performed two independent runs on the fossil-calibrated UCLN chronogram with a Markov Chain Monte Carlo (MCMC) run of 2 million generations, sampling parameters every 1000th generation. Effective sample sizes of log-likelihoods and relevant parameters were computed using the coda package in R and were >200. We plotted diversification, speciation, and extinction rate-through-time curves obtained from BAMM for all hornworts and diversification rate-through-time curves for the large genera, *Anthoceros, Dendroceros, Nothoceros, Notothylas, Phaeoceros* and *Phaeomegaceros* Duff & al., in each case accounting for incomplete taxon sampling (where only a fraction of the total species in a genus were included in the phylogenetic tree; Introduction).

■ RESULTS

Molecular clock dating and biogeography. — A ML tree from the combined data matrix (Electr. Suppl.: Fig. S1B) has solid bootstrap support for most major hornwort clades except *Phaeomegaceros*. The ages inferred under the three clock models (fossil-calibrated relaxed clock, fossil-calibrated strict clock, rate-calibrated strict clock) are shown in Table 1. They more or less agree except for the hornwort crown age, which varies from 160 (Upper Jurassic) to 229 Ma (Upper Triassic; Table 1, which shows the error ranges around all estimates). The crown ages of hornwort genera are mostly Oligocene and Miocene, and our biogeographic reconstructions only consider nodes <55 Ma, which do not much vary between clock models (Table 1).

In the biogeographic analysis (Fig. 1), *Megaceros* Campb. (11 spp., 5 included here) shows one dispersal from South Temperate regions (defined as South America, Australia and New Zealand south of 25° S lat.) to tropical Asia, namely in the ancestor of *Megaceros tjibodensis* Campb. from India (arrow

Table 1. Hornwort divergence dates (in Ma) obtained with two calibration approaches (Materials and Methods).

Calibration scheme	Root	*Antho-ceros*	*Dendro-ceros*	*Mega-ceros*	*Notho-ceros*	*Noto-thylas*	*Paraphy-matoceros*	*Phaeo-ceros*	*Phaeomega-ceros*	*Phymato-ceros*
Fossil-calibrated UCLN clock[a]	**160.19** [107.07–220]	**49.26** [31.25–70.54]	**22.6** [13.03–33.23]	**26.92** [14.85–40.0]	**28.73** [16.81–42.92]	**16.8** [8.73–26.09]	**27.21** [11.4–44.38]	**33.53** [19.27–48.44]	**18.36** [7.87–34.0]	**11.30** [2.77–22.52]
Fossil-calibrated strict clock[b]	**212.92** [175.67–272.6]	**35.21** [28.41–45.90]	**17.80** [14.24–24.21]	**25.63** [19.73–33.58]	**19.94** [15.57–26.55]	**9.84** [6.78–13.93]	**18.82** [11.98–24.63]	**19.29** [14.36–25.36]	**11.96** [7.83–16.55]	**8.15** [4.80–11.96]
Rate-calibrated strict clock[c]	**228.91** [214.69–245.16]	**37.34** [33.36–41.19]	**18.84** [15.80–21.76]	**27.44** [23.81–31.14]	**21.45** [18.46–25.49]	**10.65** [7.73–13.86]	**20.09** [15.53–24.32]	**20.37** [17.65–24.22]	**12.57** [8.67–15.46]	**8.55** [5.90–12.07]

a A log-normally distributed relaxed clock model (UCLN) calibrated with the fossil of *Notothylites nirulai* from the Deccan Intertrappean beds of Mohgaonka, India.

b A strict clock model calibrated with the same fossil.

c A strict clock model calibrated with a plastid substitution rate and a mitochondrial substitution rate for these two data partitions.

Data are mean values with 95% highest posterior density intervals shown in brackets.

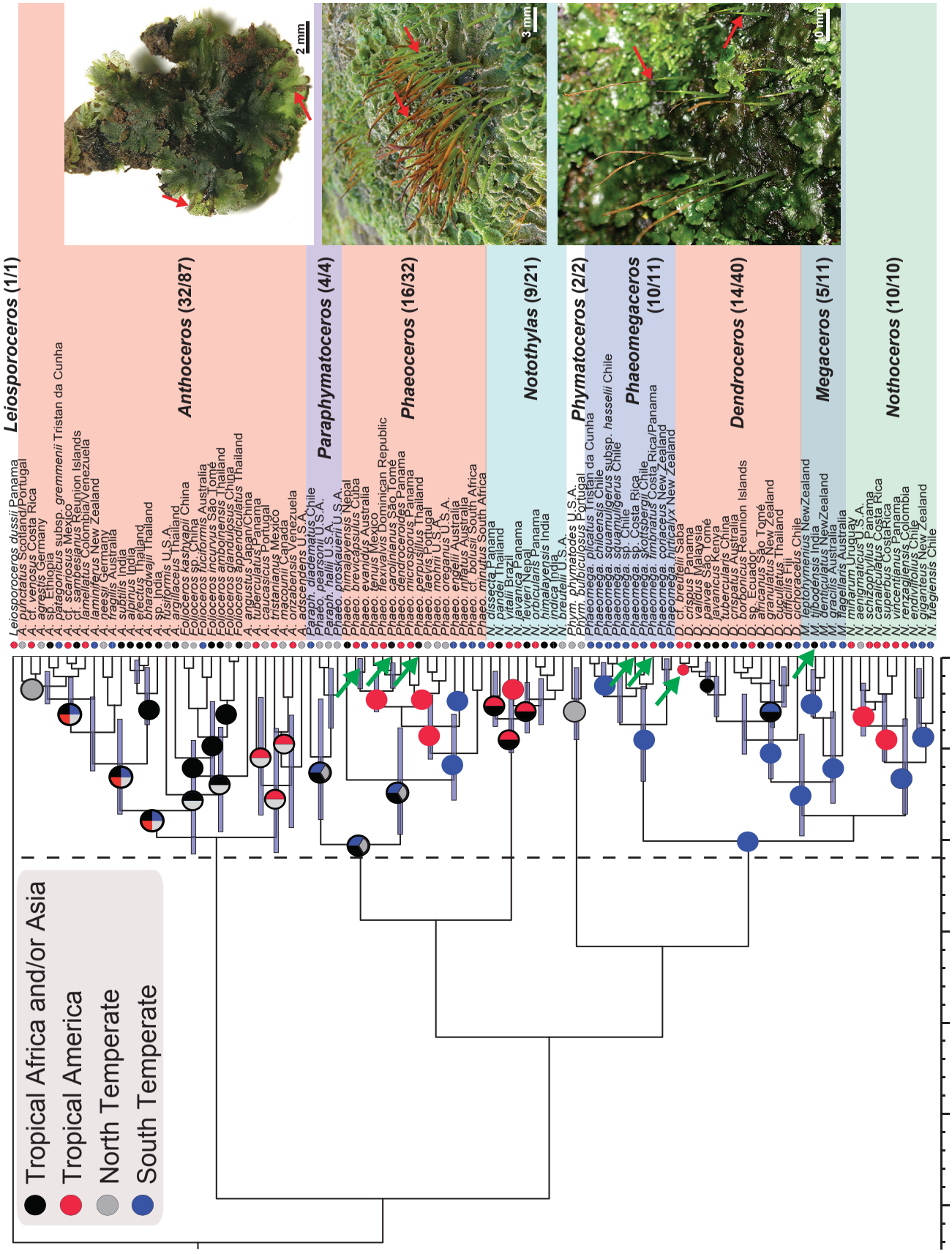

Fig. 1. A hornwort chronogram for 103 species (from 4182 aligned nucleotides of plastid and mitochondrial DNA), with ML-optimized biogeographic area reconstructions to a depth of 55 Ma. Color-coded circles next to species names indicate sample provenance; pies at nodes indicate ancestral areas. The coded areas are shown in the inset and defined in Materials and Methods. Arrows mark dispersal events discussed in the text. An ML tree from the same data with bootstrap support values is presented in Fig. S1 (Electr. Suppl.). The taxonomic identity of the genera *Paraphymatoceros* and *Folioceros* are discussed in Villarreal & al. (in press). Exemplars of hornwort species (from top): *Notothylas dissecta* Steph. (Panama), the barely exerted mature sporophytes marked by arrows; *Phaeomegaceros squamuliger* (Spruce) J.C. Villarreal (Chile) with abundant sporophytes (arrows), photo by J. Hollinger; *Nothoceros vincentianus* (Lehm. & Lindenb.) J.C.Villarreal (Costa Rica) with sporophytes in different stages of maturation (arrows). [See the online version of the paper for a full-colour illustration.]

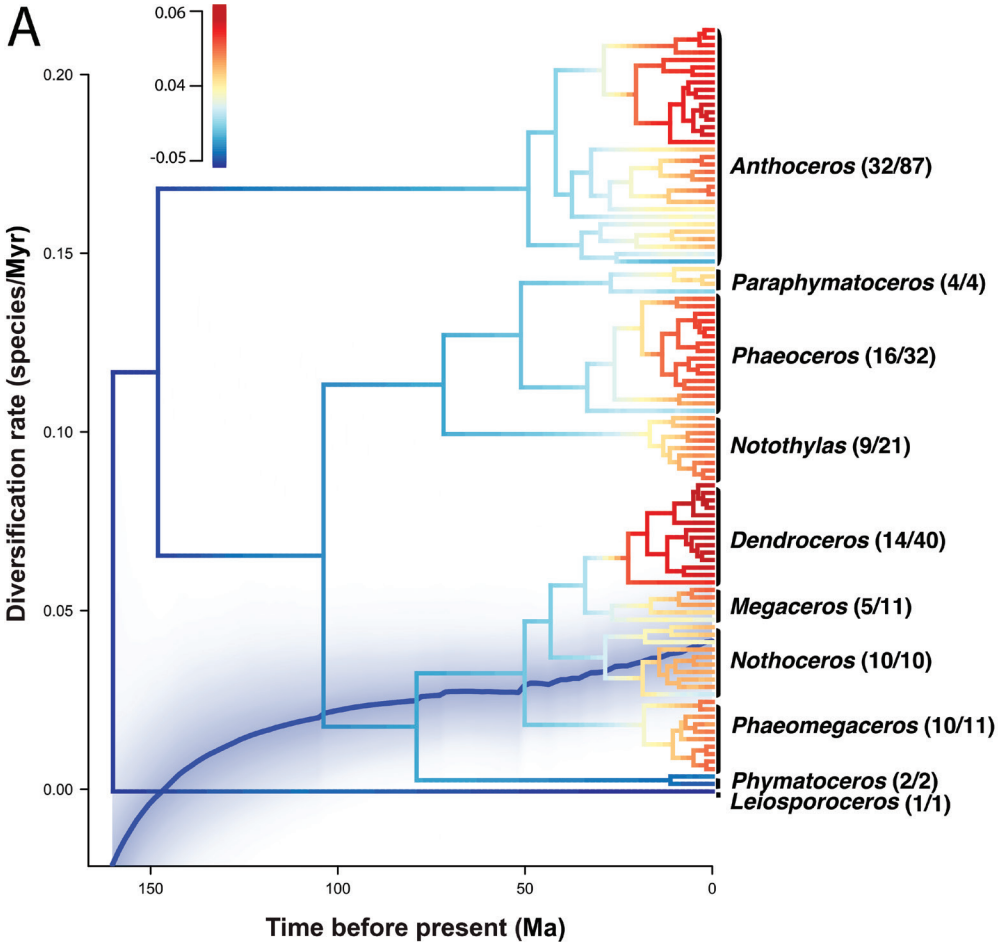

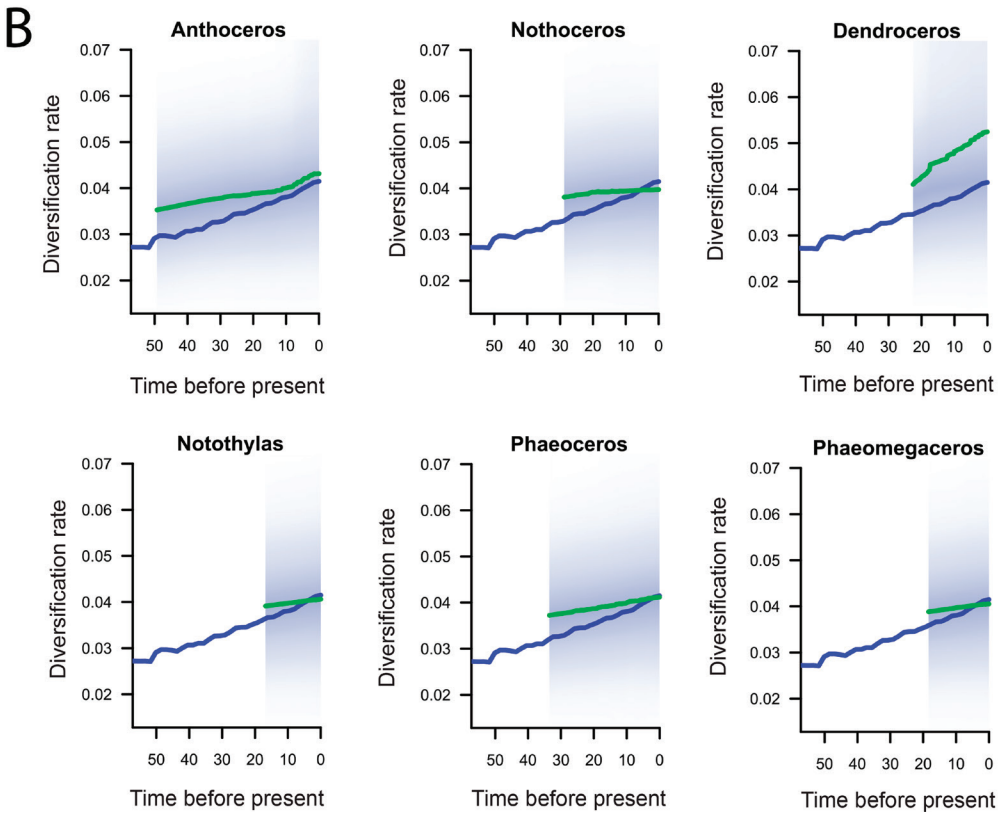

Fig. 2. A, The same hornwort chronogram as used in Fig. 1, with its branches shaded by estimated diversification rates (see inset top left), with diversification being the means of the marginal densities of the rates. The dark line (background) represents the mean diversification rate-through-time (RTT) curve across all hornworts. The intensity of the shading reflects the relative probability of the inferred diversification with upper and lower 90% Bayesian credibility intervals. **B,** The light-colour lines represent RTT plots of diversification over the past 55 Ma for six genera, the dark lines represent the hornwort background rate (same as in A), shading as in A. Note the higher diversification rates in *Anthoceros* and *Dendroceros* compared to the hornwort mean rate. [See the online version of the paper for a full-colour illustration.]

in Fig. 1). Similarly, *Dendroceros* (40 spp., 14 included here) appears to have expanded from a South Temperate ancestral region to tropical Asia and Africa, with further expansion to tropical America (defined as tropical America between 25° N and S lat.) by the ancestor of *D. breutelii* Nees and *D. crispus* (Sw.) Nees in the last 3 Myr (arrow in Fig. 1). The ancestral area of *Phaeomegaceros* (11 spp., 10 included here) is also reconstructed as South Temperate, with two dispersals to tropical America in *P. fimbriatu*s (Gottsche) Duff & al. and *Phaeomegaceros* sp. from Costa Rica (Fig. 1, arrows). The ancestral area of *Phymatoceros* Stotler & al. is reconstructed as North Temperate (e.g., Eurasia and America north of 25° N lat.); one of its two species occurs in California (*P. phymatodes* (M.Howe) Duff & al.), the other in the Mediterranean region and Macaronesia (*P. bulbiculosus* (Brot.) Stotler & al.). In *Phaeoceros* (32 spp., 16 included here), dispersal from tropical America to South Temperate Australasia (Australia) occurred in *P. evanidus* (Steph.) Cargill & Fuhrer and dispersals to tropical Africa and Asia in the ancestors of *P. carolinianus* (Michx.) Prosk. (São Tomé) and *P. perpusillus* Chantanaorr. (Thailand; Fig. 1, arrows). In *Paraphymatoceros* (4 spp., all included here), three extant species are found in California, while the fourth is the Chilean *P. diadematus* Hässel. The ancestral areas of *Anthoceros* (87 spp., 32 included here) and *Notothylas* (21 spp., 9 included here) could not be inferred unambiguously.

Diversification rates. — As inferred with BAMM under the variable-rates model (logLik = −399), hornworts have gradually increasing rates of speciation (from 0.08 to nearly 0.15 species/Myr) and a constant background extinction rate of ~0.1 species/Myr (Fig. 2; Electr. Suppl.: Fig. S1A). Diversification rates at the root are negative, but reach 0.045 species/Myr towards the present (Fig. 2A; Electr. Suppl.: Fig. S1A). No shifts in diversification rate could be detected (Fig. 2A; Electr. Suppl.: Fig. S1A). When analyzing the large genera separately, the diversification rates-through-time in *Dendroceros* and one clade within *Anthoceros* were higher than the hornwort background rate, up to 0.05 species/Myr (Fig. 2B). Under a constant-rate birth-death model (logLik = −405, i.e., less likely than the variable-rates model) the diversification rate inferred for hornworts is 0.025 species/Myr, with a speciation rate of 0.158 species/Myr, and an extinction rate of 0.133 species/Myr.

■ DISCUSSION

We investigated diversification and biogeography in hornworts, a lineage of Paleozoic origin, judging from other bryophyte lineages (mosses and liverworts) with which it may form a grade or a clade and a crown age of about 160 Ma as inferred here. The specific questions we wanted to answer concerned (1) long-distance dispersal events that have shaped post-Eocene lineage divergence and biogeography, and (2) whether available approaches for inferring diversification from DNA phylogenies would detect shifts in diversification patterns in this ancient clade. We thought this might be the case because our phylogeny includes about 102 nodes and 50% of the known species (with the missing ones added statistically; Rabosky, 2014), compared to a bryophyte-wide study that included 12 hornwort species and failed to reject a constant rate of diversification for hornworts because of a lack of statistical power (Laenen & al., 2014). In the course of the present study, we revisited our earlier hornwort chronogram (Villarreal & Renner, 2012) because the root age greatly influences inferred rates of speciation or extinction.

The crown age of hornworts. — In a study of the evolution of pyrenoids, we dated the hornwort crown group to 306 (214–399) Ma, the Upper Carboniferous (Villarreal & Renner, 2012). That high estimate was influenced by our constraint of the most recent common ancestor of the vascular plants (included as outgroups) to 416 (±3) Ma. Specifically, we had included nine vascular plants, one moss, and one liverwort. The inclusion of such sparse outgroups violates a basic assumption of Bayesian dating approaches, namely even taxon sampling across lineages (Drummond & Bouckaert, 2015). In the present study, we therefore chose not to include outgroups, rooting instead on a single species of hornworts that may be the sister to the remaining species. Hornwort rooting is unlikely to greatly affect our biogeographic analyses because we only consider nodes <55 Ma that would hardly change with different rooting (Electr. Suppl.: Fig. S1). The hornwort crown age of 160 (107–220) Ma obtained here (with the fossil-calibrated relaxed clock model) obviously differs greatly from our previous estimate.

Our new results are supported by the cross-validation of at least two of the inferred node ages against fossil ages that were not used as calibration points. First, there is an *Anthoceros* spore from the Lower Cretaceous Baqueró Formation, Argentina (Archangelsky & Villar de Seone, 1996). The Lower Cretaceous ranges from 145 to 100 Ma (Gradstein & Ogg, 2012), but isotope dating of the fossil-bearing stratum indicates an Aptian age (Cladera & al., 2002), that is, 125–113 Ma. The split between *Anthoceros* s.l. and the remaining hornworts is here estimated at 148 Ma (Fig. 1), and the fossil is thus a bit younger, suggesting that its morphology represents a taxon on, or sister to, the stem of *Anthoceros*. Second, there is a *Phaeomegaceros* spore from the Lower Miocene Uscari Formation, Costa Rica (Graham, 1987; the Lower Miocene ranges from 23 to 13 Ma; Gradstein & Ogg, 2012). The age inferred for the crown group of *Phaeomegaceros* with our clock model is 18 Ma (Fig. 2A; Table 1), which falls in the middle of the age of the geological formation in which the fossil was found. Lastly, our fossil-calibrated relaxed clock model yielded a crown age of *Nothoceros* of 29 (17–43) Ma, which fits with the age estimated earlier using a plastid rate calibration of 35 (30–40) Ma (Villarreal & Renner, 2014).

Biogeography. — Hornworts, like other spore-producing plants, have high dispersal capabilities, and the ranges of some species, such as *Nothoceros vincentianus* (Lehm. & Lindenb.) J.C. Villarreal from Mexico to Costa Rica and on Guadeloupe and Martinique, which molecular data support as monophyletic (Villarreal & Renner, 2014), seem to reflect this. It is doubtful, however, that all such trans-oceanic species are monophyletic, and much more sequencing work is necessary to test current species circumscriptions. Several surprising dispersal events

inferred here, such as those in *Dendroceros* and *Phaeoceros* (Fig. 1, arrows), need to be regarded with caution because we only included 14 of the 40 species of the former genus and 16 of the 32 species of the latter. For the genus *Nothoceros*, which comprises ten species (all sampled), nine in the Americas and one in New Zealand (*N. giganteus*), the present global analyses confirmed our earlier inference that the ancestor of *Nothoceros* was South Temperate and expanded its range to eastern North America, with an early long-distance dispersal from New Zealand to Chile sometime during the Miocene (Villarreal & Renner, 2014).

Figure 2 shows inferred ancestral regions only to a time depth of about 55 Ma because of vastly different continental positions and climates prior to the Eocene. At that time depth, we reconstruct the most recent common ancestor of the *Nothoceros/Phaeomegaceros* clade as "South Temperate", which may be trustworthy, given that this inference is driven mostly be the modern ranges of relatively well-sampled genera *Megaceros*, *Nothoceros*, and *Phaeomegaceros*. Nevertheless, such reconstructions should probably be met with skepticism because we are basically treating range as an inherited character. Current modeling approaches in historical biogeography, whether the Mk1 model used here or the dispersal-extinction-cladogenesis model implemented in the software LAGRANGE (Smith & Ree, 2010; Ree, 2013), all assume that geographic range change is anagenetic and has nothing to do with speciation (interruption of gene flow), a fact that has been underappreciated (Matzke, 2013, 2014). Much more work is needed in this area before one places too much weight on likelihoods for this or that ancestral range that derive from implausible reconstruction approaches.

Absence of shifts in diversification and constant background extinction: limited modeling power. — Our BAMM analyses inferred a steadily increasing rate of diversification for the entire hornworts (up to 0.045 species/Myr; Fig. 2), and similar to Laenen & al. (2014), we were unable to detect any shifts in diversification. We did detect higher than average rates in some hornwort genera, however, such as the epiphytic genus *Dendroceros* (with a crown age of ~22 Ma, Fig. 2B, and a diversification rate of 0.041 to 0.052 species/Myr). This increase may be linked to the availability of an angiosperm-dominated canopy, similar to what has been inferred for ferns, mosses, and the liverwort order Porellales (Schuettpelz & Pryer, 2009; Fiz-Palacios & al., 2011; Feldberg & al., 2014). However, the models used in these studies to link traits to changes in diversification rates all have statistical problems because of pseudoreplication (Maddison & Fitzjohn, 2015; Rabosky & Goldberg, 2015). A problem relevant to the present attempt to infer diversification rates in hornworts is that diversification models in BAMM all assume that each species—regardless of its age—has the same instant speciation probability (under the Yule tree process) or the same instant speciation and extinction probability (under the birth-death tree process model). This amazingly unrealistic assumption probably invalidates all published diversification rates (Hagen & al., 2015).

A final caveat for our study of diversification rates is the uncertainty surrounding the crown age of hornworts. As discussed above, using vascular plant outgroups and several fossils, we earlier inferred a hornwort crown age of 306 (214–399) Ma (Villarreal & Renner, 2012), while we here infer a crown age of 160 (107–220) Ma, with a single-fossil-calibrated relaxed clock model and without outgroups. Since the root age greatly influences the global diversification rate, our hornwort-wide rates should be regarded with caution.

Conclusions. — We present the first global analysis of hornwort biogeography and diversification. As expected, dispersal has played a prominent role in hornwort geographical distribution, and this may become even more apparent once sampling within species is increased to test if transcontinental species are monophyletic. That this may not be the case is suggested by a study of spore patterns and DNA sequences in Australian and New Zealand *Megaceros*, using multiple specimens per species, which showed that while spore patterns were indistinguishable, none of the New Zealand species are conspecific with any Australian species (Cargill & al., 2013). Such cryptic species may increase the current estimate of 220 species of hornworts worldwide. Lastly, our finding of constant and extremely low extinction rates and no significant global diversification rate shifts supports Rabosky's (2014) warning about the low power of current approaches to infer extinction and ancient changes in diversification.

■ ACKNOWLEDGMENTS

For plant material we thank T. Peng and R.-L. Zhu (East China Normal University), S. Chantanaorrapint (Songkla University, Thailand), D.C. Cargill (Australian National Herbarium, CANB), S. Pressel and J.G. Duckett (Natural History Museum, London). Financial support came from the DFG grant RE 603/14-1.

■ LITERATURE CITED

Alfaro, M.E., Santini, F., Brock, C., Alamillo, H., Dornburg, A., Rabosky, D., Carnevale, G. & Harmong, J.L. 2009. Nine exceptional radiations plus high turnover explain species diversity in jawed vertebrates. *Proc. Natl. Acad. Sci. U.S.A.* 106: 13410–13414. http://dx.doi.org/10.1073/pnas.0811087106

Archangelsky S. & Villar de Seone, L. 1996. Estudios palinógicos de la formación Baqueró (Cretácico), provincia de Santa Cruz, Argentina. *Ameghiniana* 35: 7–19.

Asthana, A.K. & Srivastava, S.C. 1991. Indian hornworts: A taxonomic study. *Bryophyt. Biblioth.* 42: 1–158.

Cargill, D.C., Vella, N.G.F., Sharma, I. & Miller, J.T. 2013. Cryptic speciation and species diversity among Australian and New Zealand hornwort taxa of *Megaceros* (Dendrocerotaceae). *Austral. Syst. Bot.* 26: 356–377. http://dx.doi.org/10.1071/SB13030

Chitaley, S.D. & Yawale, N.R. 1980. On *Notothylites nirulai* gen. et sp. nov.: A petrified sporogonium from the Deccan-Intertrappean beds of Mohgaonkalan M. P. (India). *Botanique* 9: 111–118.

Cladera, G., Andreis, R., Archangelsky, S. & Cúneo, R. 2002. Estratigrafía del grupo Baqueró, Patagonia (provincia de Santa Cruz, Argentina). *Ameghiniana* 39: 1–20.

Cox, C.J., Li, B., Foster, P.G., Embley, T.M. & Civán, P. 2014. Conflicting phylogenies for early land plants are caused by composition biases among synonymous substitutions. *Syst. Biol.* 63: 272–279. http://dx.doi.org/10.1093/sysbio/syt109

Cusimano, N. & Renner, S.S. 2010. Slowdowns in diversification rates from real phylogenies may not be real. *Syst. Biol.* 59: 458–464. http://dx.doi.org/10.1093/sysbio/syq032

Cusimano, N., Stadler, T. & Renner, S.S. 2012. A new method for handling missing species in diversification analysis applicable to randomly or nonrandomly sampled phylogenies. *Syst. Biol.* 61: 785–792. http://dx.doi.org/10.1093/sysbio/sys031

Drummond, A.J. & Bouckaert, R.R. 2015. *Bayesian evolutionary analysis with BEAST 2*. Cambridge: Cambridge University Press.

Drummond, A.J., Suchard, M.A., Xie, D. & Rambaut, A. 2012. Bayesian phylogenetics with BEAUti and the BEAST 1.7. *Molec. Biol. Evol.* 29: 1969–1973. http://dx.doi.org/10.1093/molbev/mss075

Duff, R.J., Villarreal, J.C., Cargill, D.C. & Renzaglia, K.S. 2007. Progress and challenges toward developing a phylogeny and classification of the hornworts. *Bryologist* 110: 214–243. http://dx.doi.org/10.1639/0007-2745(2007)110[214:PACTDA]2.0.CO;2

Feldberg, K., Schneider, H., Stadler, T., Schäfer-Verwimp, A., Schmidt, A.R. & Heinrichs, J. 2014. Epiphytic leafy liverworts diversified in angiosperm-dominated forests. *Nat. Sci. Rep.* 4: 5974. http://dx.doi.org/10.1038/srep05974

Fiz-Palacios, O., Schneider, H., Heinrichs, J. & Savolainen, V. 2011. Diversification of land plants: Insights from a family-level phylogenetic analysis. *B. M. C. Evol. Biol.* 11: 341. http://dx.doi.org/10.1186/1471-2148-11-341

FitzJohn, R.G., Maddison W.P. & Otto S.P. 2009. Estimating trait-dependent speciation and extinction rates from incompletely resolved phylogenies. *Syst. Biol.* 58: 595–611. http://dx.doi.org/10.1093/sysbio/syp067

Gaut, B.S. 1998. Molecular clocks and nucleotide substitution rates in higher plants. *Evol. Biol.* 30: 93–120.

Gradstein, F.M. & Ogg, G. 2012. The chronostratigraphic scale. Pp. 31–42 in: Gradstein, F.M., Ogg, J.G., Schmitz, M. & Ogg, G.M. (eds), *The geologic time scale 2012*. Oxford: Elsevier. http://dx.doi.org/10.1016/B978-0-444-59425-9.00002-0

Graham, A. 1987. Miocene communities and paleoenvironments of southern Costa Rica. *Amer. J. Bot.* 74: 1501–1518. http://dx.doi.org/10.2307/2444045

Hagen, O., Hartmann, K., Steel, M. & Stadler, T. 2015. Age-dependent speciation can explain the shape of empirical phylogenies. *Syst. Biol.*, epub ahead of print. http://dx.doi.org/10.1093/sysbio/syv001

Hasegawa, J. 1980. Taxonomical studies on Asian Anthocerotae. II. Some Asian species of *Dendroceros*. *J. Hattori Bot. Lab.* 47: 287–309.

Karol, K.G., Arumuganathan, K., Boore, J.L., Duffy, A.M., Everett, K.D.E., Hall, J.D., Hansen, S.K., Kuehl, J.V., Mandoli, D.F., Mishler, B.D., Olmstead, R.G., Renzaglia, K.S. & Wolf, P.G. 2010. Complete plastome sequences of *Equisetum arvense* and *Isoetes flaccida*: Implications for phylogeny and plastid genome evolution of early land plant lineages. *B. M. C. Evol. Biol.* 10: 321. http://dx.doi.org/10.1186/1471-2148-10-321

Laenen, B., Shaw, B., Schneider, H., Goffinet, B., Paradis, E., Désamoré, A., Heinrichs, J., Villarreal, J.C., Gradstein, S.R., McDaniel, S.F., Long, D.G., Forrest, L.L., Hollingsworth, M.L., Crandall-Stotler, B., Davis, E.C., Engel, J., von Konrat, M., Cooper, E.D., Patino, J., Cox, C.J., Vanderpoorten, A. & Shaw, A.J. 2014. Extant diversity of bryophytes emerged from successive post-Mesozoic diversification bursts. *Nat. Commun*. 5: 6134. http://dx.doi.org/10.1038/ncomms6134

Maddison, W.P. & FitzJohn, R.G. 2015. The unsolved challenge to phylogenetic correlation tests for categorical characters. *Syst. Biol.* 64: 127–136. http://dx.doi.org/10.1093/sysbio/syu070

Maddison, W. P. & Maddison, D.R. 2010. Mesquite: A modular system for evolutionary analysis, version 2.73. http://mesquiteproject.org

Maddison, W.P., Midford, P.E. & Otto, S.P. 2007. Estimating a binary character's effect on speciation and extinction. *Syst. Biol*. 56: 701–710. http://dx.doi.org/10.1080/10635150701607033

Matzke, N. J. 2013. Probabilistic historical biogeography: New models for founder-event speciation, imperfect detection, and fossils allow improved accuracy and model-testing. *Frontiers Biogeogr.* 5: 242–248.

Matzke, N.J. 2014. Model selection in historical biogeography reveals that founder-event speciation is a crucial process in island clades. *Syst. Biol*. 63: 951–970. http://dx.doi.org/10.1093/sysbio/syu056

Muñoz, J., Felicisimo, A.M., Cabezas, F., Burgaz, A.R. & Martínez, I. 2004. Wind as a long-distance dispersal vehicle in the Southern Hemisphere. *Science* 304: 1144–1147. http://dx.doi.org/10.1126/science.1095210

Palmer, J.D. 1991. Plastid chromosome, structure and evolution. Pp. 5–53 in: Bogorad, L. & Vasil, I.K. (eds.), *The molecular biology of plastids*. San Diego: Academic Press.

Piippo, S. 1993. Bryophyte flora of the Huon Peninsula, Papua New Guinea. LIV. Anthocerotophyta. *Acta Bot. Fenn.* 148: 27–51.

Proskauer, J. 1948. Studies on the morphology of *Anthoceros* I. *Ann. Bot. (Oxford)* 12: 237–265.

Qiu, Y.-L., Lia, L., Wanga, B., Chen, Z., Knoop, V., Groth-Malonek, M., Dombrovska, O., Lee, J., Kent, L., Rest, J., Estabrook, G.F., Hendry, T.A., Taylor, D.W., Testa, C.M., Ambros, M., Crandall-Stotler, B., Duff, R.J., Stech, M., Frey, W., Quandt, D. & Davis, C.C. 2006. The deepest divergences in land plants inferred from phylogenomic evidence. *Proc. Natl. Acad. Sci. U.S.A.* 103: 15511–15516. http://dx.doi.org/10.1073/pnas.0603335103

Rabosky, D.L. 2014. Automatic detection of key innovations, rate shifts, and diversity dependence on phylogenetic trees. *PLOS ONE* 9(2): e89543. http://dx.doi.org/10.1371/journal.pone.0089543

Rabosky, D.L. & Goldberg, E. 2015. Model inadequacy and mistaken inferences of trait-dependent speciation. *Syst. Biol.* 64: 340–355. http://dx.doi.org/10.1093/sysbio/syu131

Rambaut, A. 2014. Figtree: A graphical viewer of phylogenetic trees. http://tree.bio.ed.ac.uk/software/

Rambaut, A., Suchard, M. & Drummond, A. 2014. Tracer, version 1.6.0. http://tree.bio.ed.ac.uk/software/tracer/

Ree, R.H. 2013. Lagrange configurator, version 20130526 (beta). http://www.reelab.net/lagrange/configurator/index (last accessed 7 Aug 2014).

Renzaglia, K.S., Villarreal, J.C. & Duff, R.J. 2009. New insights into morphology, anatomy and systematics of hornworts. Pp. 139–171 in: Goffinet, B. & Shaw, A.J. (eds.), *Bryophyte biology*, ed. 2. Cambridge: Cambridge University Press.

Schneider, H., Schuettpelz, E., Pryer, K.M., Cranfill, R., Magallón, S. & Lupia, R. 2004. Ferns diversified in the shadow of angiosperms. *Nature* 428: 553–557. http://dx.doi.org/10.1038/nature02361

Schuettpelz, E. & Pryer, K.M. 2009. Evidence for a Cenozoic radiation of ferns in an angiosperm-dominated canopy. *Proc. Natl. Acad. Sci. U.S.A.* 106: 11200–11205. http://dx.doi.org/10.1073/pnas.0811136106

Scotese, C.R. 2001. *Atlas of Earth history*. Arlington, Texas: University of Texas.

Smith S.A. & Ree R.H. 2010. Lagrange: Likelihood analysis of geographic range evolution. https://code.google.com/p/lagrange/ (last accessed 7 Aug 2014).

Stamatakis, A., Hoover, P. & Rougemont, J. 2008. A rapid bootstrap algorithm for the RAxML web servers. *Syst. Biol.* 57: 758–771. http://dx.doi.org/10.1016/j.jtbi.2009.07.018

Villarreal, J.C. & Renner, S.S. 2012. Hornwort pyrenoids, a carbon-concentrating mechanism, evolved and were lost at least five times during the last 100 million years. *Proc. Natl. Acad. Sci. U.S.A.* 109: 18873–18878. http://dx.doi.org/10.1073/pnas.1213498109

Villarreal, J.C. & Renner, S.S. 2013. Correlates of monoicy and dioicy in hornworts, the apparent sister group to vascular plants. *B. M. C. Evol. Biol.* 13: 239. http://dx.doi.org/10.1186/1471-2148-13-239

Villarreal, J.C. & Renner, S.S. 2014. A review of molecular-clock calibrations and substitution rates in liverworts, mosses, and hornworts, and a timeframe for a taxonomically cleaned-up genus *Nothoceros*. *Molec. Phylogen. Evol.* 78: 25–35. http://dx.doi.org/10.1016/j.ympev.2014.04.014

Villarreal, J.C., Forrest, L.L., Wickett, N. & Goffinet, B. 2013. The plastid genome of the hornwort *Nothoceros aenigmaticus*: Phylogenetic signal in inverted repeat expansion, pseudogenization and intron gain. *Amer. J. Bot.* 100: 467–477. http://dx.doi.org/10.3732/ajb.1200429

Villarreal, J.C., Cargill, D.C., Hagborg, A., Söderström, L. & Konrat, M. von In press. Notes on early land plants. 61. Taxonomic changes in hornworts. *Phytotaxa*.

Wicket, N.J., Mirarab, S., Nguyen, N., Warnow, T., Carpenter, E., Matasci, N., Ayyampalayam, S., Barker, M.S., Burleigh, J.G., Gitzendanner, M.A., Ruhfel, B.R., Wafula, E., Der, J.P., Graham, J.W., Mathews, S., Melkonian, M., Soltis, D.E., Soltis, P.S., Miles, N.W., Rothfels, C.J., Pokorny, L., Shaw, A.J., DeGironimo, L., Stevenson, D.W., Surek, B., Villarreal, J.C., Roure, B., Philippe, H., dePamphilis, C.W., Chen, T., Deyholos, M.K., Baucom, R.S., Kutchan, T.M., Augustin, M.M., Wang, J., Zhang, Y., Tian, Z., Yan, Z., Wu, X., Sun, X., Wong, G.K.-S. & Leebens-Mack, J. 2014. A phylotranscriptomic analysis of the origin and early diversification of land plants. *Proc. Natl. Acad. Sci. U.S.A.* 111: E4859–E4868. http://dx.doi.org/10.1073/pnas.1323926111

Appendix 1. Voucher and GenBank accession numbers (in the sequence *rbcL*, *nad5*, *trnK-matK*, *rps4*) for accessions used in this study. Collector(s), collection number, herbarium and provenance are provided. Accession numbers of new sequences are given in bold.

Anthoceros adscendens Lehm. & Lindenb., *Hays 4201-3* (M), U.S.A. (Florida), KF482293, KF482250, –, **KP238761**; ***Anthoceros agrestis*** Paton, *Villarreal 1353* (M), Germany, **KP238681, KP238678, KP238675, KP238684;** ***Anthoceros alpinus*** Steph., *Duckett IW110* (M), India, KF482268, KF482243, KF482215, **KP238685;** ***Anthoceros angustus*** Steph., *Zhang 7704* (SZG), China, AB086179.1, JF815561.1, AB086179.1, AB086179.1; ***Anthoceros argillaceus*** (Steph.) Verdoorn, *Chantanaorrapint 2737A* (PSU), Thailand, **KP238682, KP238679, KP238676, KP238707;** ***Anthoceros bharadwajii*** Udar & Asthana, *Chantanaorrapint 229* (PSU), Thailand, KF482267, KF482242, KF482214, **KP238686;** ***Anthoceros caucasicus*** Steph., *Garcia s.n.* (M), Portugal, JX872419, JX872453, KF482294, **KP238687;** ***Anthoceros erectus*** Kash., *Chantanaorrapint 212, 550* (PSU), Thailand, KF482269, –, KF482216, **KP238689;** ***Anthoceros fragilis*** Steph., *Lovatt & Holland TH 9821* (CANB), Australia, KF482270, KF482244, KF482298, –; ***Anthoceros fusiformis*** Aust., *Doyle 11347* (ABSH, M), U.S.A. (California), DQ845677, DQ845727.1, KF482217, –; ***Anthoceros lamellatus*** Steph., *Duckett s.n.* (ABSH), Venezuela, *Rincon s.n.* (M), Colombia, DQ845679, JX872455, KF482299, **KP238690;** ***Anthoceros laminiferus*** Steph., *Duckett s.n.* (ABSH), *Slack 211056* (M), New Zealand, KF482271, DQ845728.1, KF482300, **KP23869;** ***Anthoceros macounii*** M.A.Howe, *Faubert s.n.* (M, QFA), Canada, JX872421, JX872456, KF482301, **KP238692;** ***Anthoceros neesii*** Prosk., *Manzke s.n.* (M), Germany, JX872422, JX872457, KF482302, **KP238693;** ***Anthoceros orizabensis*** (Steph.) Hässel, *Villarreal 770* (M), Venezuela, JX872423, JX872458, KF482303, **KP238694;** ***Anthoceros patagonicus*** subsp. ***gremmenii*** J.C.Villarreal & al., *Gremmen 2005-T028* (F), Tristan de Cunha, JX872424, JX872459, KF482304, **KP238695;** ***Anthoceros punctatus*** L., *Sergio s.n.* (LISU, M) Portugal, *Chamberlain & Kungu s.n* (E), Scotland, KF482272, DQ845730, KF482305, **KP238696;*****Anthoceros*** cf. ***sambesianus*** Steph., *Serousiaux s.n.* (M), Reunion Islands, JX872425, JX872460, KF482295, –; ***Anthoceros*** cf. ***scariosus*** Aust., *Villarreal 1217* (M), Mexico, JX872420, JX872454, KF482296, –; ***Anthoceros* sp.1. Ethiopia,** *Hylander 4504* (M), Ethiopia, KF482273, KF482245, KF482306, **KP238697;** ***Anthoceros* sp.2 India,** *Duckett IW57* (BM), India, KF482274, –, KF482218, **KP238698;** ***Anthoceros subtilis*** Steph., *Villarreal 1236A* (M), India, –, –, –, **KP238699;** ***Anthoceros tristanianus*** J.C.Villarreal & al., *Villarreal 1032* (M), Tristan de Cunha, JX872426, JX872461, KF482219, **KP238700;** ***Anthoceros tuberculatus*** Lehm. & Lindenb., *Villarreal & Rodríguez 857* (CONN), Panama, JX872427, JX872462, KF482307, –; ***Anthoceros*** cf. ***venosus*** Lindenb. & Gottsche, *Salazar & al. 20654* (PMA), Costa Rica, JX872428, JX872463, KF482297, **KP238688;** ***Dendroceros africanus*** Steph., *Shevock 39829* (M), São Tomé, KF482276, KF482252, KF482220, –; ***Dendroceros borbonicus*** Steph., *Theo Arts 153-51* (BR), Reunion Islands, KF482277, KF482253, KF482221, –; ***Dendroceros*** cf. ***breutelii*** Nees, *Buck 51344* (NY), Saba, JX872429, JX872464, KF482309, –; ***Dendroceros cichoraceus*** (Mont.) Gottsche, *Larraín 31162* (CONC), Chile, JX872430, JX872465, KF482310, **KP238701;** ***Dendroceros crispatus*** (Hook.) Nees, *Cargill 28* (CANB), *Paterson s.n. B570* (CANB), Australia, AY463048, DQ845708.1, KF482311, –; ***Dendroceros crispus*** (Sw.) Nees, *Villarreal 1296* (M), Panama, JX885633, KF482254, KF482312, **KP238702;** ***Dendroceros cucullatus*** Steph., *Chantanaorrapint 1623* (PSU), Thailand, KF482275, KF482251, KF482308, –; ***Dendroceros difficilis*** Steph., *Von Konrat s.n.* (FM), Fiji, HM056148.1, JX872466, JN559927.1, **KP238703;** ***Dendroceros granulatus*** (Mitt.) Steph., *Duckett s.n.* (ABSH), *Cargill DAM-KI 130* (CANB), New Zealand, AY463049, –, KF482222, –; ***Dendroceros javanicus*** (Nees) Nees, *Buchbender s.n.* (CONN), Kenya, JX872431, JX872467, KF482313, **KP238704;** ***Dendroceros paivae*** Garcia & al., *C. Garcia ST 125* (LISU 237201), São Tomé, JX872432, JX872468, KF482314, **KP238705;** ***Dendroceros* sp.,** *Gradstein 12106* (DUKE), Ecuador, KF482278, KF482255, KF482223, –; ***Dendroceros tuberculatis*** Hatt., *Shevock 39039* (M), China, KF482279, KF482256, KF482224, –; ***Dendroceros validus*** Steph., *Duckett D27* (M), Malaysia, JX885634, –, **KP238673**, –; ***Folioceros amboinensis*** (Schiffn.) Steph., *Chantanaorrapint 2493* (PSU), Thailand, KF482280, KF482246, KF482315, KP238706; ***Folioceros appendiculatus*** (Steph.) J.Haseg., *Chantanaorrapint 1884* (PSU), Thailand, **KP238683, KP238680, KP238677,** –; ***Folioceros fuciformis*** (Mont) D.C.Bharadwaj., *Cargill s.n.* (CANB), Australia, KF482281, DQ845726.1, KF482316, **KP238708;** ***Folioceros glandulosus*** (Lehm. & Lindenb.) D.C.Bharadwaj, *Zhang 5622* (SZG), China, JF815573.1, JF815563.1, –, –; ***Folioceros incurvus*** (Steph.) D.C.Bharadwaj, *Shevock 39742* (M), São Tomé, KF482282, KF482247, KF482225, **KP238709;** ***Folioceros kashyapii*** Udar & Srivastava, *Peng 20111015-85* (HSNU), China, KF482283, KF482248, KF482226, **KP238710;** ***Folioceros* sp.,** *Peng 20111016-3* (HSNU), China, KF482284, KF482249, KF482227, **KP238711;** ***Leiosporoceros dussii*** (Steph.) Hässel, *Villarreal & Araúz 851, 1285* (PMA), Panama, AY463052.1, AY894803.1, KF482228, **KP238712;** ***Megaceros denticulatus*** (Steph.), *Duckett s.n.* (ABSH), New Zealand, AY463038, DQ845705, –, –; ***Megaceros flagellaris*** (Mitt.) Steph., *D.C. Cargill 885* (CANB), Australia, GQ845371, GQ845372.1, JN559929, **KP238713;** ***Megaceros gracilis*** (Reichardt) Steph., *Fuhrer s.n., D.C. Cargill B10, PW 235B* (CANB), Australia, AY463039, JX872469, **KP238674,** –; ***Megaceros leptohymenius*** (Hook.f. & Tayl.) Steph., *Duckett 3N-117, 3N36* (M), New Zealand, JX885636, KF482258, KF482230, **KP238714;** ***Megaceros tjibodensis*** Campb., *Ducket IE52* (M), India, KF482286, KF482259, KF482231, –; ***Nothoceros aenigmaticus*** (R.M.Schust.) J.C.Villarreal & McFarland, *Villarreal & McFarland 935* (CONN), U.S.A. (Tennessee), GQ504731, GQ504735, KC285889, KC285889; ***Nothoceros canaliculatus*** (Pagan) J.C.Villarreal & al., *Lepiz s.n.* (M), Costa Rica, HM056176.1, JX872470, JN559952.1, **KP238716;** ***Nothoceros endiviifolius*** (Mont). J.Haseg., *Duckett s.n.* (CONN), Chile, DQ845645, GQ504737, JN559930.1, **KP238717;** ***Nothoceros fuegiensis*** (Steph.) J.C.Villarreal, *Goffinet 9527* (CONN), Chile, HM056156, DQ097162, JN559934, **KP238718;** ***Nothoceros giganteus*** (Lehm. & Lindenb.) J.Haseg., *Engel & Von Konrat 27407* (M), New Zealand, HM056154, DQ845709, JN559932, **KP238719;** ***Nothoceros minarum*** (Nees) J.C.Villarreal, *Cargill & Prieto 2625* (CANB), Uruguay, JX872433, JX872471, KF612916, **KP238720;** ***Nothoceros renzagliensis*** J.C.Villarreal & al., *Villarreal & al. 1080* (COL), Colombia, HM056162.1, JX872472, JN559940, **KP238721;** ***Nothoceros schizophyllus*** (Steph.) J.C.Villarreal, *Villarreal & Varela 584* (PMA), Panama, GQ504732, GQ504736, JN559949.1, **KP238722;** ***Nothoceros superbus*** J.C.Villarreal & al., *Salazar & al. 20676* (PMA), Costa Rica, HM056172.1, JX872473, KF482317, **KP238723;** ***Nothoceros vincentianus*** (Lehm. & Lindenb.) J.C.Villarreal, *Villarreal & Rodrıguez 840* (CONN), *Villarreal & al. 641* (ABSH), Panama, HM056171, DQ845711, JN559943, **KP238724;** ***Notothylas breutelii*** (Gottsche) Gottsche, *Krayeski s.n.*, cultured (ABSH), U.S.A., AY463054, DQ845719, KF482318, **KP238725;** ***Notothylas dissecta*** Steph., *Araúz & al. 798* (M, PMA), Panama, JX872434, JX872474, KF482319, **KP238726;** ***Notothylas himalayensis*** Udar & Singh, *Ducket IW56* (M), India, KF482287, KF482260, KF482232, **KP238727;** ***Notothylas indica*** Kashyap, *Ducket IE38* (M), Panama, KF482288, KF482261, KF482233, **KP238728;** ***Notothylas javanica*** (Sande Lac.) Gottsche, *Villarreal 806* (PMA), *Villarreal 1311* (M), Panama, JX885638, DQ845720, KF482320, **KP238729;** ***Notothylas levieri*** Steph. ex Schiffn., *Long 30668* (E), Nepal, JX872436, JX872475, KF482234, **KP238730;** ***Notothylas orbicularis*** (Schwein.) Sull ex A.Gray, *Villarreal & al. 1302* (M), Panama, JX885639, KF482262 , –, **KP238731;** ***Notothylas pandei*** Udar & Chandra, *Chantanaorrapint 1666* (PSU), Thailand, KF482289, KF482263, KF482235, –; ***Notothylas vitalii*** Singh, *Gradstein s.n.* (PER), Brazil, JX872437, JX872476.1, –, –; ***Paraphymatoceros diadematus*** Hässel, *Larraín 34069* (CONC), Chile, JX872438, JX872477, KF482321, **KP238732;** ***Paraphymatoceros hallii*** (Aust.) Hässel, *Doyle 11363* (ABSH), U.S.A. (California), DQ845670, JX872478, KF482236, **KP238733;** ***Phaeoceros*** cf. ***bolusii*** (Sim) S.Arnell, *Hedderson 16894* (BOL), South Africa, JX872440, JX872481, KF482324, **KP238736;** ***Phaeoceros brevicapsulus***

Appendix 1. Continued.

(Steph.) Hässel, *Queralta s.n.* (M), Cuba, JX872439, JX872480, –, –; ***Phaeoceros carolinianus*** (Michx.) Prosk., *Shevock 39775* (M), São Tomé, KF482290, KF482264, KF482237, –; ***Phaeoceros dendroceroides*** (Steph.) Hässel, *Villarreal 1305* (M), Panama, KF482291, KF482265, KF482325, **KP238737;** ***Phaeoceros engelii*** Cargill & Fuhrer, *Cargill & Fuhrer 1015* (CANB), Australia, JX872441, JX872482, KF482326, **KP238738;** ***Phaeoceros evanidus*** (Steph.) Cargill & Fuhrer, *Cargill 875* (CANB), Australia, JX872442, JX872483, KF482327, **KP238739;** ***Phaeoceros flexivalvis*** (Nees & Gottsche) Hässel, *Villarreal 863* (M), Dominican Republic, JX872443, JX872484, KF482238, **KP238740;** ***Phaeoceros himalayensis*** (Kash.) Prosk., *Long 30423* (E), Nepal, JX872444, JX872485, KF482239, **KP238741;** ***Phaeoceros inflatus*** (Steph.) Hässel, *Cargill & Fuhrer 474* (CANB), Australia, JX872445, JX872486, KF482328, **KP238742;** ***Phaeoceros laevis*** (L). Prosk., *Sergio s.n.* (LISU), Portugal, DQ845673, DQ845721, KF482240, **KP238743;** ***Phaeoceros microsporus*** (Steph.) Hässel, *Villarreal 725* (M), Panama, JX872446, JX872487, KF482329, **KP238744;** ***Phaeoceros minutus*** (Steph.) S.Arnell, *Hedderson 16879* (BOL), South Africa, JX872447, JX872488, KF482330, **KP238745;** ***Phaeoceros mohrii*** (Aust.) Hässel, *Doyle 11341* (M), U.S.A. (California), DQ845672, DQ845724, KF482331, –; ***Phaeoceros oreganus*** (Aust.) Hässel, *Doyle 11382* (M), U.S.A. (California), DQ845661, JX885644, KF482332, **KP238746;** ***Phaeoceros pearsonii*** (M.A.Howe) Prosk., *Doyle s.n.* (M), U.S.A. (California), DQ845668.1, AY894802.1, KF482322, **KP238734;** ***Phaeoceros perpusillus*** S.Chantanaorrapint, *Chantanaorrapint 1551* (PSU), Thailand, KF482292, KF482266, KF482333, **KP238747;** ***Phaeoceros proskauerii*** Stotler & al., *Doyle 11339* (ABSH), U.S.A. (California), EU283415.1, JX872479, KF482323, **KP238735;** ***Phaeoceros tenuis*** (Spruce) Hässel, *Ibarra Morales 17* (FCME), Mexico, JX872448, –, KF482334, **KP238748;** ***Phaeomegaceros chiloensis*** (Steph.) J.C.Villarreal, *Larraín 34061* (CONC), Chile, JX872449, JX872489, –, **KP238749;** ***Phaeomegaceros coriaceus*** (Steph.) Duff & al., *Glenny 9757* (CONN), New Zealand, JX872450, JX872490, KF482335, **KP238750;** ***Phaeomegaceros fimbriatus*** (Gottsche) Duff & al., *Villarreal 779* (ABSH), Panama, *Villarreal & al. 881* (CONN), Costa Rica, HM056149, DQ845716, JN559928, **KP238752;** ***Phaeomegaceros hirticalyx*** (Steph.) Duff & al., *Duckett s.n.* (ABSH, M), AY463043, DQ845713, KF482336, **KP23875;** ***Phaeomegaceros plicatus*** (Mitt) J.C.Villarreal, Engel & Vana, *Gremmen T07-1097* (F), Tristan de Cunha, JX872451, JX872491, KF482337, **KP238753;** ***Phaeomegaceros skottsbergii*** (Steph.) Duff & al., *Cuvertino s.n.* (SGO), *Larraín 31354* (CONN), Chile, DQ845659, DQ845715, –, **KP238755;** ***Phaeomegaceros*** **sp. nov. 1,** *Villarreal & al. 871* (M), Costa Rica, JX872452, JX872492, KF482338, **KP238754;** ***Phaeomegaceros*** **sp. nov. 2,** *Duckett s.n.* (ABSH), Chile, DQ 845651, DQ845714, KF482339, **KP238756;** ***Phaeomegaceros squamuligerus*** (Spruce) J.C.Villarreal, *Jofre s.n.* (CONN), Chile, HM038430, HM038432, KF482340, **KP238757;** ***Phaeomegaceros squamuligerus*** subsp. ***hasselii*** J.C.Villarreal, *Goffinet 7106* (CONN), Chile, HM038429, HM038431, KF482341, **KP238758;** ***Phymatoceros bulbiculosus*** (Brot.) Stotler & al., *Sergio s.n.* (LISU), Portugal, DQ268978.1, DQ097163.1, KF482241, **KP238759;** ***Phymatoceros phymatodes*** (M.A.Howe) Duff & al., *Doyle s.n*, *Doyle 11480* (ABSH, M), U.S.A. (California), DQ845660.1, DQ845717.1, KF482342, **KP238760.**